The University of Akron
IdeaExchange@UAkron

College of Polymer Science and Polymer Engineering

9-22-2005

Effect of Thermal Transport on Spatiotemporal Emergence of Lamellar Branching Morphology During Polymer Spherulitic Growth

Haijun Xu

Wirunya Keawwattana

Thein Kyu
University of Akron Main Campus, tkyu@uakron.edu

Please take a moment to share how this work helps you through this survey. Your feedback will be important as we plan further development of our repository.
Follow this and additional works at: http://ideaexchange.uakron.edu/polymer_ideas

 Part of the Polymer Science Commons

Recommended Citation
Xu, Haijun; Keawwattana, Wirunya; and Kyu, Thein, "Effect of Thermal Transport on Spatiotemporal Emergence of Lamellar Branching Morphology During Polymer Spherulitic Growth" (2005). *College of Polymer Science and Polymer Engineering*. 47.
http://ideaexchange.uakron.edu/polymer_ideas/47

This Article is brought to you for free and open access by IdeaExchange@UAkron, the institutional repository of The University of Akron in Akron, Ohio, USA. It has been accepted for inclusion in College of Polymer Science and Polymer Engineering by an authorized administrator of IdeaExchange@UAkron. For more information, please contact mjon@uakron.edu, uapress@uakron.edu.

Effect of thermal transport on spatiotemporal emergence of lamellar branching morphology during polymer spherulitic growth

Haijun Xu, Wirunya Keawwattana, and Thein Kyu[a)]
Department of Polymer Engineering, The University of Akron, Akron, Ohio 44325

(Received 14 June 2005; accepted 22 July 2005; published online 27 September 2005)

Spatiotemporal emergence of lamellar branching morphology of polymer spherulite has been investigated theoretically in the framework of a phase field model by coupling a crystal solidification potential pertaining to a nonconserved crystal order parameter with a temperature field generated by latent heat of crystallization. A local free-energy density having an asymmetric double well has been utilized to account for a first-order phase transition such as crystallization. To account for the polymorphous nature of polymer crystallization, the phase field order parameter of crystal at the solidification potential of the double-well local free-energy density is modified to be supercooling dependent. The heat conduction equation, incorporating liberation of latent heat along the nonuniform solid-liquid interface, has led to directional growth of various hierarchical structures including lamella, sheaflike structure, and spherulite. Two-dimensional calculations have been carried out based on experimentally accessible material parameters and experimental conditions for the growth of syndiotactic polypropylene spherulite. The simulations illustrate that, under self-generated thermal field, the initial nucleus is anisotropic having lamellar stacks that transforms to a sheaflike structure and eventually to a lamellar branching morphology with a dual-eye-pocket texture at the core. It appears that the released latent heat is responsible for the lamellar side branching and splaying from the main lamellae. On the same token, the heat build-up seemingly prevents the interface boundaries of neighboring spherulites from over running on each other during impingement, thereby forming the grain boundary. © *2005 American Institute of Physics*.
[DOI: 10.1063/1.2036976]

INTRODUCTION

It is well documented that polymer single crystals are generally grown from dilute solutions, whereas more complicated hierarchical crystalline morphologies such as axialite, hedrite, and spherulite emerge from the melt or concentrated solutions.[1] Recently, it becomes apparent that various single crystals can be grown from the melt. The existence of supramolecular structures is not unique to polymers, but such organizations have been found in a large variety of small molecule systems such as inorganic substances, bioorganisms, and metals.[2] In general, spherulite has been characterized as a rounded aggregate of radiating lamellar crystals with a fibrous appearance which originates from a nucleus such as a particle of contaminant, catalyst residue, or fluctuation in density created by chance. These structures often grow through stages—first, lamellar needles, then lamellar bundles, and sheaflike lamellar aggregates, and finally the spherulites with lamellar branching which may range in diameter from submicrons to several hundred microns.[1,3] In the case of polymers, spherulites may be conveniently discerned under a polarized optical microscope, which consist of a large number of lamellae growing radially outward from a primary nucleus at the core. Often some lamellae may be twisted about their long axes, which result in the concentric bands or spiral structures.[4–6] The spherical shape arises usually due to side branching and splaying of microstructures,[7,8] while such a structure in the initial to intermediate stages may not be spherical, but rather resembles a sheaflike morphology.

In the polymer spherulitic growth, the melt-crystallized lamellae often stack into bundles from a single nucleation site and grow radially outward until they impinge on the neighboring lamellar stacks growing from other nucleating sites. The lamellar stacks are laterally constrained to some extent, so that they form a ribbonlike structure. The lateral constraint instability is perceived to develop from impurities at the growing lamellar sides. Impurities include a number of things such as dirt, chain segments of improper tacticity, branched segments, end groups, and other amorphous components that cannot crystallize at the temperature of crystallization. However, some of these amorphous chains may crystallize at a lower temperature to facilitate a secondary crystallization occurring in the interlamellar or interspherulitic regions, creating branching points that allow the spherulite to grow into a three-dimensional object.

Although the main lamellae grow in some preferential crystallographic axis, e.g., *b* axis in polyolefin, the side branching in a spherulite is noncrystallographic unlike the dendrites in small molecule systems. In low-molecular weight materials such as snowflakes or ice crystallites, branching predominantly occurs along low index crystallographic planes. In polymeric spherulites with the lamellae radiating from the core, the lamellar orientation is random

[a)]Author to whom correspondence should be addressed. Electronic mail: tkyu@uakron.edu

 © 2005 American Institute of Physics

globally, and thus there exists little or no relationship between the crystallographic planes and the direction of branching. The release of latent heat gives a temperature distribution along the crystal-melt interface, resulting in a nonuniform boundary having density fluctuations, some of which eventually serve as likely sites for nucleation of lamellar branching.

The primary objective of the present paper is to elucidate the lamellar branching mechanisms during the growth of polymer spherulites experimentally as well as theoretically based on a modified phase field model. In the phase field model, the interface is treated to be smooth having a small but finite thickness. A phase field order parameter ψ, hereafter called a crystal order parameter defined as the ratio of folded chain length over optimum length, i.e., the linear crystallinity, is introduced in order to distinguish the ordered solid phase from the disordered liquid by locally identifying each phase at a particular point in space and time. An advantage of this approach is that there is no requirement for tracking the boundary of the interface, as opposed to the free boundary problems encountered in the sharp interface approaches.[9] One of the characteristics of polymer crystals, which distinguish themselves from other crystallizable materials, is that the polymer crystals are inherently imperfect due to chain defects. To explain the metastable polymorphic nature of the crystalline polymers, a crystal order parameter at the solidification potential has been modified to depend on the temperature of crystallization. In this approach, the system is defined as a spatiotemporal field of a crystal order parameter ψ that possesses a value of zero in the melt state and a finite value in the metastable crystalline state in a manner dependent on supercooling. The spatiotemporal evolution of the simulated spherulitic texture has been compared with the experimental observation of syndiotactic polypropylene (sPP).

EXPERIMENTAL SECTION

Syndiotactic polypropylene was kindly supplied by FINA Chemical and Oil Company. The weight average and number average molecular weight of sPP were reported to be 174 000 and 74 700, respectively, with a polydispersity of 2.3. A solution of sPP was prepared by dissolving it in hot xylene controlled at ~100 °C and then the solution mixtures were spread on glass slides. To ensure the complete removal of the solvent, the glass slides were immersed in distilled water (nonsolvent) for 1 h, and dried at ambient temperature, and then further dried in a vacuum oven at room temperature for additional two days. All experiments were carried out after maintaining the samples at 160 °C for 10 min. This procedure was done to give the same thermal history to all samples and to further remove residual solvent if any. The thickness of the sample films used for optical microscopy was approximately 10 μm.

The morphology was analyzed using an optical microscope (Nikon Optishot 2-POL). The light source was a Halogen bulb operated at 12 V and 100 W. The sample heating chamber (Mettler FP82 HT) interlinked to a programmable temperature controller (Mettler Toledo FP90 Central processor) was utilized to control the temperature. Optical micrographs were obtained by using a 35-mm camera (Nikon, FX-35DX) connected to an automatic exposure time controller (Nikon, UFX-DX). The film exposure time was automatically controlled through the transmitted light intensity. Real time observations of the change in morphology with temperature were observed using a color digital camera (Sony, HyperHAD), interfaced with a personal computer. Asymmetrix digital video acquisition software was used to analyze the digital image.

THEORETICAL SCHEME

In the phase field modeling,[10–14] the total free energy of the nonconserved system is defined in terms of a combination of a local free-energy density and a nonlocal gradient term, viz.,

$$F(\psi) = \int f_{\text{cryst}}(\psi) d\Omega = \int [f_{\text{local}}(\psi) + f_{\text{grad}}(\psi)] d\Omega, \qquad (1)$$

where $\psi(r,t)$ represents the crystal order parameter at time t and position r. The temporal evolution of the crystal phase order parameter is described in the framework of time-dependent Ginzburg-Landau (TDGL) theory, model A equation,[12] as

$$\frac{\partial \psi(r,t)}{\partial t} = -\Gamma \frac{\delta F(\psi)}{\delta \psi(r,t)}, \qquad (2)$$

where Γ is related to the rotational mobility which is inversely proportional to the viscosity or the frictional force.

As demonstrated by Chan,[14] the local free energy of solidification may be expressed in accordance with the Landau expression[13] in powers of the order parameter ψ as $f_{\text{local}} = A\psi^2 + B\psi^3 + C\psi^4 + \ldots$. In order for the Landau free energy to be applicable to a first-order phase transition, it is necessary for the coefficient of the third power term to be finite, i.e., $B \neq 0$. This free energy is characterized by an asymmetric double well that involves metastability and latent heat. However, when the coefficient of the third power term, B, is exactly zero, such free energy, having a symmetric double well, is applicable to a second-order phase transition or the first-order transition only at the node.[14]

In polymer crystallization,[15,16] the crystal melting temperature obtained at a given crystallization condition is significantly different from that of the equilibrium melting point. It is therefore important to consider various metastable solid states in polymer solidifications that revealed various hierarchy morphologies such as disordered spherulites to highly ordered single crystals. To account for the metastability and defective polymer crystals, multiple energy minima reflecting the chain-folding steps have been proposed in the literature.[16]

In the present case, the metastability of polymer crystallization may be explicable simply through an appropriate modification of the phase field model by treating the order parameter at the solidification potential to be crystallization/melting temperature dependent, i.e., $\zeta_0 = T_m / T_m^0$. T_m^0 is the equilibrium melting temperature, whereas T_m represents the melting temperature that is obtained from a given crystalli-

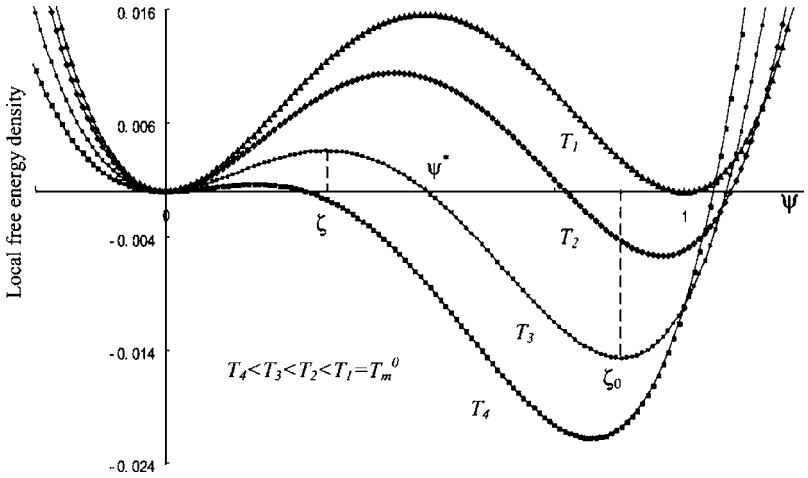

FIG. 1. Variation of the local free-energy density as a function of crystal order parameter ψ for various temperatures showing different nucleation barrier heights and locations, ζ. The crystal state $\psi=\zeta_0$ varies with the crystallization temperature indicating the imperfection of polymer crystals.

zation temperature T. Physically, ζ, which is defined as the ratio of the folded chain length and the optimum folded chain length, represents the linear crystallinity and thus its value is bound between the limits of zero representing melt and unity representing the crystal at equilibrium. In view of the supercooling-dependent solidification potential, ζ_0 would be less than one which in turn implies that the polymer crystals are not perfect containing sizable defects or amorphous materials.

In the present modified phase field model, the local free-energy density of the system is treated as a continuous function of temperature $T(r,t)$, having the form of an asymmetric double well with respect to ψ,

$$f_{\text{local}}(\psi,T) = W\int_0^{\psi}\psi(\psi-\zeta)(\psi-\zeta_0)d\psi,$$

$$= W\left[\frac{\zeta\zeta_0}{2}\psi^2 - \frac{\zeta+\zeta_0}{3}\psi^3 + \frac{\psi^4}{4}\right], \tag{3}$$

where ζ is related to the supercooling ΔT, and W is a dimensionless coefficient describing the height of the energy barrier to overcome for nucleation, i.e., the penalty for nucleation. As shown in Fig. 1, the stable solid can vary from some finite values of ζ_0 to unity at equilibrium depending on the supercooling or the melting temperature. At $T_m^0(\zeta=0.5)$, the free-energy density has an identical local minimum meaning the crystal and melt can coexist. When $T<T_m^0(\zeta<0.5)$, the free-energy density has a global minimum at $\zeta_0<1$, i.e., the linear crystallinity is less than unity, which suggests that the emerged crystals contain some defects or amorphous materials reflecting the polymorphous nature of the polymer crystals. Nonetheless, the metastable crystal phase is more stable than the unstable melt. Hence, the melt will solidify by overcoming the nucleation barrier peak labeled by ζ on the ψ axis. As the supercooling increases, ζ_0 shifts to a lower value less than unity, which means that the emerged crystal is imperfect containing sizable defects. The advantage of the present approach is that there is no need for considering the multiple metastable wells to account for the metastability potentials of polymer crystallization, a simple free-energy double well with various (supercooling/melting temperature dependent) ζ_0 would serve the same purpose without losing the physical essence of the general solidification phenomenon.

In addition, the nonlocal free-energy density can be written in terms of the gradient free-energy density describing the growth process as

$$f_{\text{grad}}(\psi) = \tfrac{1}{2}\kappa^2\cdot(\nabla\psi)^2, \tag{4}$$

where κ is the interface gradient coefficient which is treated as scalar for simplicity.

Substituting Eqs. (2)–(4) into Eq. (1) leads to

$$\frac{\partial\psi(r,t)}{\partial t} = -\Gamma\frac{\partial F(\psi)}{\partial\psi}$$
$$= -\Gamma[W\psi(\psi-\zeta)(\psi-\zeta_0) - \kappa^2\nabla^2\psi] + \eta(\psi). \tag{5}$$

Physically, the first term on the right-hand side of Eq. (5) represents the nucleation, i.e., the surface nucleation to be more precise, whereas the second term signifies the growth, i.e., propagation of the crystal-melt interface. The last term corresponds to the thermal force term of Eq. (A10), which is operative only at the solid-melt interface. The phase field of crystal solidification commonly occurs in conjunction with other fields such as self-generated temperature or mechanical deformation fields despite the fact that crystallization is taking place under quiescent condition. In the case of binary blends, a concentration field may be added to describe the competition between the phase separation and crystallization of the constituent(s). Derived from the conservation law of enthalpy, the heat equation, which involves the liberation of latent heat, may be expressed as

$$\rho C_p\frac{\partial T}{\partial t} = k_T\nabla^2 T + \rho\Delta H_u\frac{\partial\psi}{\partial t}, \tag{6}$$

where $\rho(\text{kg/m}^3)$ is density, $C_p(\text{kJ/kg K})$ heat capacity, $k_T(\text{J/m s K})$ thermal conductivity, and $\Delta H_u(\text{J/kg})$ latent heat of the pure substance. Let thermal diffusivity $\alpha=k_T/\rho C_p$, $K=\Delta H_u/C_p$, then the heat conduction equation for the temperature evolution is simplified as follows:

$$\frac{\partial T}{\partial t} = \alpha \nabla^2 T + K \frac{\partial \psi}{\partial t}. \tag{7}$$

In practice, when the crystallization temperature is lowered or the supercooling is increased, the orderness of the emerging structure is far from perfection, and thus its local degree of crystallinity would be lowered. Although ΔH_u of a pure substance is constant, its value for a polymer crystal would be strongly dependent on crystallinity, crystal morphology and imperfection. Since these morphological parameters depend on the crystallization temperature, i.e., K may be supercooling dependent through heat of fusion of polymer crystals, i.e., $K=\Delta H_u/C_p \propto \Delta T$. As cautioned by Kobayashi, this K should not be regarded as the true supercooling; K value should be estimated directly from the heat of fusion and heat capacitance whenever possible. However, it is often the case that these thermal quantities were not determined experimentally for each crystallization temperature, and thus ΔT (or K) may be taken as $(T_m - T_c)$ for the purpose of qualitative comparison, where T_c is the experimental temperature of crystallization. It should be emphasized that K is kept constant during the course of isothermal crystallization at a given supercooling.

It can be anticipated that the exothermic latent heat thus generated during crystallization would be accumulated at the concave curvature regions, where further growth is prohibited. At the convex tips, the heat can be dissipated readily into the undercooled melt. Such differing trends of latent heat liberation destabilize the crystal-melt interface, thereby rendering the complex interface morphologies.

In order to afford a better quantitative comparison between the computations and the experiments, the model parameters Γ, W, ζ, and κ must be related to the experimentally accessible physical/material parameters as demonstrated by Allen and Cahn.[17] These supercooling-dependent model parameters were expressed in what follows:[18]

$$\psi^* = \frac{T_m^0 - T_m}{T_m^0 - T}, \quad \zeta = \frac{4\zeta_0\psi^* - 3\psi^{*2}}{6\zeta_0 - 4\psi^*}, \tag{8}$$

$$W = 6\frac{\Delta H_u}{nRT\zeta_0^3}\left(\frac{T_m - T}{T_m^0}\right)\left(\frac{\zeta_0}{2} - \zeta\right)^{-1}, \tag{9}$$

$$\kappa = 6\frac{\sigma}{nRT}\left(\frac{2}{W}\right)^{1/2}. \tag{10}$$

It should be emphasized that these model parameters are supercooling dependent, and thus any variations in the crystallization (e.g., experimental temperature of crystallization) would effectively alter their values.

Considering one-dimensional propagation of the interface with a moving frame of reference under a uniform velocity of $\nu = \partial\psi/\partial t$ at equilibrium, Eq. (5) leads to

$$\kappa^2 \frac{d^2\psi}{dx^2} + \frac{\nu}{\Gamma}\frac{d\psi}{dx} - \frac{\partial f}{\partial \psi} = 0. \tag{11}$$

We seek a solution of the form $\psi = \psi(z)$, where $z = x - \nu t$ under the boundary condition of the traveling wave as $\psi \to \zeta_0$ when $x \to -\infty$ and $\psi \to 0$ when $x \to +\infty$,[19] one obtains a stationary solution

$$\psi(z) = \frac{\psi_0}{\left[1 + \exp\left(z\zeta_0\sqrt{\frac{W}{2\kappa^2}}\right)\right]}, \tag{12}$$

with the selected velocity

$$\nu = -\Gamma\kappa\left(\zeta - \frac{\zeta_0}{2}\right)\sqrt{W}. \tag{13}$$

Combining Eqs. (9), (10), and (13) results in

$$\Gamma = \frac{\sqrt{2}}{12}\nu\left[\frac{\sigma}{nRT}\left(\frac{\zeta_0}{2} - \zeta\right)\right]^{-1}. \tag{14}$$

In order to present the governing Eqs. (5) and (7) in dimensionless forms, the variables are rescaled with dimensionless time τ and dimensionless variables denoted with tilde symbols as follows: $\tilde{x} = x/d^*$, $\tilde{y} = y/d^*$, and $\tau = Dt/d^{*2}$, where $d^* = 1 \times 10^{-7}$ m is the characteristic length and $D = 2.1 \times 10^{-10}$ m^2/s is the linear diffusion coefficient of sPP.[20] The final governing equations are represented in dimensionless forms by rescaling temperature as $u = (T - T_c)/(T_m - T_c)$,

$$\frac{\partial \psi}{\partial \tau} = -[W\psi(\psi - \zeta_0)(\psi - \zeta) - \tilde{\kappa}_0^2\tilde{\nabla}^2\psi] + \eta(\psi), \tag{15}$$

$$\frac{\partial u}{\partial \tau} = \tilde{\alpha}\tilde{\nabla}^2 u - \tilde{K}\frac{\partial \psi}{\partial \tau}, \tag{16}$$

where $\tilde{\nabla} = \tilde{i}(\partial/\partial\tilde{x}) + \tilde{j}(\partial/\partial\tilde{y})$, $\tilde{\kappa}_0 = (\Gamma\kappa)/(Dd^*)$, $\Gamma = D/d^{*2}$, $\tilde{\alpha} = \alpha/d^{*2}\Gamma$, and $\tilde{K} = \Delta H_u/C_p T_m$. In practice, all of the above model parameters can be accessible through experimentally measurable quantities.

To elucidate the behavior of crystallization in binary blends, another time-evolution equation, e.g., Cahn-Hilliard equation[21] pertaining to the blend concentration having Flory-Huggins free energy[22] has been added to couple with the current nonconserved phase field equation. Such a model is known as the TDGL model C. This model has been used in simulating crystallization in metal alloys[23,24] and spherulitic growth in polymer blends.[25] But for a miscible system where the phase separation is insignificant, the equation pertaining to concentration may be ignored.

RESULTS AND DISCUSSION

Equations (15) and (16) have been solved numerically in two dimensions on a square lattice using a central finite difference method for spatial discretization and an explicit forward difference for time steps with a no-flux boundary condition. Now the challenge is whether the modified phase field model could capture the emergence of lamellar branching morphology of spherulites. Various grid sizes (512×512 and 1024×1024) and temporal steps have been employed to ascertain the stability of the simulation. In order to avoid overcrowding of the nuclei, firstly, a single thermal perturbation is imparted to trigger a nucleation event at the center, which is the basis for interfacial genesis. Once an interface is

TABLE I. Model parameters calculated from experimentally determined material parameters of sPP at a given experimental temperature of 100 °C.

Material parameters	Model parameters
$\Delta H_u = 8.0$ kJ/mol[a]	
$T_m^0 = 160$ °C[a]	$W = 9.07$
$C_p = 0.0265$ kJ/(mol K)[a]	$\kappa^2 = 5.62 \times 10^{-14}$ m^2
$k_T = 0.220$ J/(m s K)[a]	$\zeta = 0.3$
$\sigma = 0.0221$ J/m^2[a]	$\alpha = 4.03 \times 10^{-7}$ m^2/s
$\rho = 907$ kg/m^3[a]	$K = 302$ K
$\Gamma = 10^4 - 10^5$ s^{-1}	$\Gamma = 10^5$ s^{-1}
$T_m = 129$ °C[b]	
$T_c = 100$ °C	[a,b]

[a]Reference 20.
[b]Reference 33.

formed, the crystal grows in a manner that is governed by the interface diffusion in conjunction with the local chemical-potential difference across the interface.

During the spherulite growth of polymer materials, the crystal-melt interface having a finite thickness is rather coarse and irregular. As demonstrated by Kobayashi,[10] a small noise term $\eta(\psi) = \mu\psi(1-\psi)$ may be imparted on the solid-melt interface to generate the rough interface, where μ is the amplitude of the perturbation term. According to Beckerman *et al.*,[26] the local free-energy density of solidification having a similar perturbation term can be deduced from a first principle such as the Gibbs-Thomson equation. As shown in the Appendix, the thermal force may be modified for polymer crystallization as $\eta(\psi) = \mu\psi(\zeta_0 - \psi)$, where $\mu = (\mu_k/\delta)(T_m - T)$. For the purpose of demonstrating the emerged dense branching morphology (or spherulite) at a given crystallization temperature of 100 °C, the values of the model parameters as deduced from the materials parameters and the experimental conditions of syndiotactic polypropylene (sPP) were listed in Table I. In literature, the value of the rotational mobility, Γ varies significantly from 10^{11} for metal alloys[19] to 10^2 for a polyethylene solid crystal.[27] As evidenced in the C^{13} nuclear magnetic resonance (NMR) study, the rotational mobility Γ is of the order of 10^5 for the loose loops at the lamellar surface of polyethylene crystals.[28] At present, the experimental value of Γ of sPP is not available, but it may be estimated from the relationship $\Gamma = D/d^{*2}$. Using the characteristic length $d^* = 1 \times 10^{-7}$ m, and the translational diffusion coefficient of sPP as $D = 2.1 \times 10^{-10}$ m^2/s (Ref. 20) that gives Γ of 2.1×10^4 s. This value would be higher at the solid-melt interface and thus it is fair to estimate the order of magnitude to be somewhat comparable to that of PE at the interface (e.g., 10^5). Except for this estimated rotational mobility at the solid-melt interface of sPP, all model parameters in Table I are specific to the sPP under consideration. Note that the values of these model parameters are specific to a given crystallization temperature of 100 °C, but would change with supercooling through Eqs. (8)–(14).

As illustrated in Fig. 2(a), the liberated latent heat at the convex crystalline tips diffuses away into the undercooled melt, whereas at the concave regions, the heat is seemingly trapped as there is virtually no thermal gradient between the

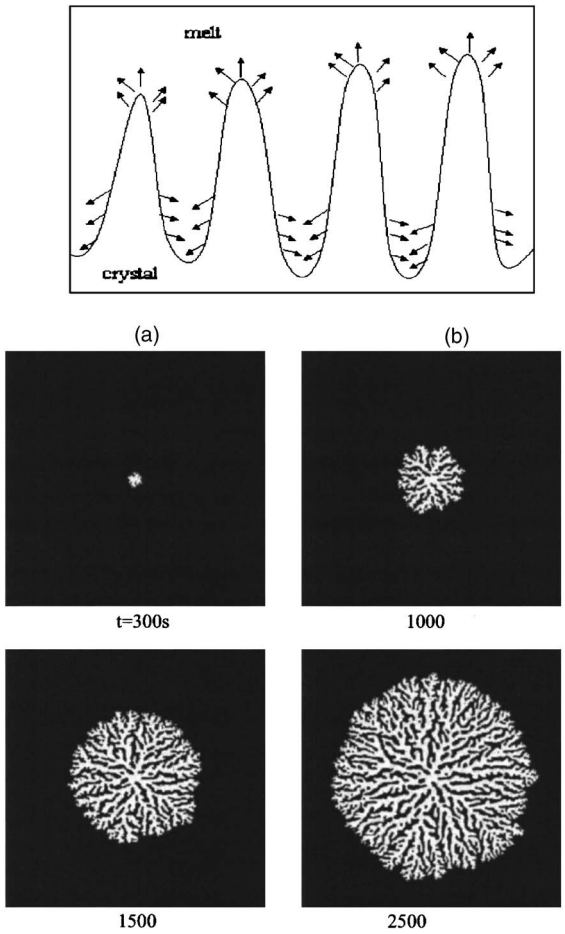

FIG. 2. (a) Schematic drawing of latent heat generation at the crystal-melt interface. The arrows indicate directions of the heat flow. (b) The spatiotemporal growth of sPP spherulite crystallized at 100 °C in the crystal order-parameter field showing the regular dense lamellar branching morphology. The model parameters used were listed in Table I with the amplitude of noise $a = 0.01$ and the grid size of 512×512. The length scale of the frame is 51.2 μm.

two neighboring walls for the heat to diffuse away, thereby preventing further crystal growth. Figure 2(b) showed the simulated results of the regular lamellar branching morphology of sPP spherulitic growth. Usually such spherulitic growth occurs at a deeper supercooling, whereas faceted single crystals form predominantly at shallow supercooling. In deep quenching, the emerged melt-crystal boundary is rough, and even small amplitude of the irregular interface is amplified by the latent heat liberated. By virtue of the non-uniform thermal transport, the lamellae undergo directional growth through extensive tip splitting and side branching from the main lamellae, which eventually evolve into the seaweed, alternatively known as dense branching morphology, under such self-generated temperature field.

At a moderate supercooling, the lamellar structure developed from the onset of nucleation seemingly evolve faster along the long lamellar axes relative to the transverse direction because of the differential growth rates corresponding to the crystallographic axes. As can be witnessed in Fig. 3, these individual lamellae are anisotropic and tend to stack on each other at the nucleating stage. These lamellar stacks continue to grow predominantly along the long axes because the

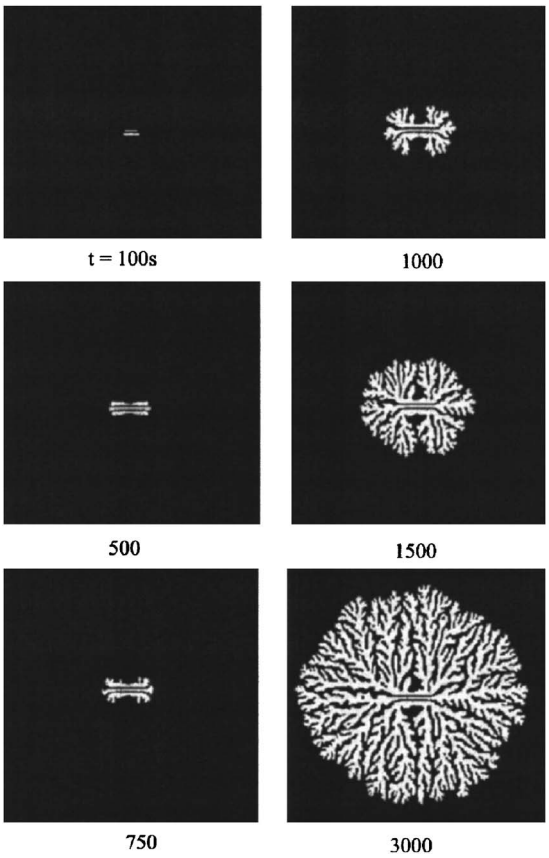

FIG. 3. Spatiotemporal growth of sPP spherulite crystallized at 100 °C in the crystal order-parameter field, showing the sheaflike structure. The calculation was undertaken using the model parameters listed in Table I with the amplitude of noise $a=0.01$ and the grid size of 512×512. The length scale of the picture frame is 51.2 μm.

lateral growth is hindered by the presence of the neighboring lamellae. When these stacked lamellae reach a certain length, the ones at the most outer sides tend to curve toward the outer free space. With continued growth, the multilayer crystals splay out progressively while additional lamellar side branching takes place from the branches, and eventually form the sheaflike structure. These lamellae were locally anisotropic; however, the overall structure becomes isotropic in a global sense with the progression of the spherulitic growth.

Recently, Granasay *et al.*[29] demonstrated the impurities (heterogeneity) induced crystal solidification resulting in the dense lamellar branching morphology or polymer spherulites using the combination of the phase field order parameter and the orientation order parameter. In the present case, the heterogeneity is triggered by the thermal fluctuation associated with latent heat liberation at the crystal-melt interface boundary. Hence the coupling with the heat conduction equation is essential although the phase field equation (A10) for crystal solidification was derived from the Gibbs-Thomson equation. The coupled phase field equations are certainly capable of predicting a diverse body of morphologies, encompassing the irregular seaweed type to the regular dendrite as well as the faceted growth. The morphology transitions from the faceted hexagonal single crystal to snow-flake structures (or dendrites), then to dense lamellar morphology (or seaweed) have been found experimentally in ultrathin films of isotactic polystyrene single crystals under various crystallization temperatures.[30] These experimental observations on the morphology landscape can be explicable theoretically in the framework of the present approach in terms of the supercooling and the growth anisotropy.[31] Moreover, the present phase field approach is the first to theoretically demonstrate the spatiotemporal emergence of the sheaflike structure with a so-called dual-eye-pocket that has been frequently observed in the spherulitic growth of other polymeric materials.[1–4] It should be emphasized that the lamellar branching and splaying can occur from a nucleus that contains a single lamella in forming the sheaflike texture.[32] That is to say, the lamellar stacking at the nuclei is an interesting observation, but it is not a necessary criterion for side branching and/or splaying in forming a sheaf.[12]

In practice, heterogeneous necleation occurs in polymer crystallization. The multinucleation event was triggered in the crystal order-parameter field based on the large density fluctuations driven by thermal perturbation. As can be witnessed in the experiment[33,34] as well as in the simulation,[32] some nuclei that exceeded the critical size grow while other diminishes. In the simulation, the anisotropic lamellar growth is maintained for some initial period, but it looses its character with progressive growth as manifested in the time sequence of the emerging sheaflike and regular spherulites [Fig. 4(a)]. When the neighboring spherulites impinge on each other, the growth ceases and concurrently grain boundaries appear between these neighboring spherulites. The formation of grain boundaries may be attributed to the latent heat being released into the interstitial spherulitic regions where the heat is seemingly accumulated, thereby preventing further growth of the spherulites. Consequently, the impinged spherulites transform into polyhedral in shape.

The simulated trends of spherulitic growth can be confirmed in the isothermal crystallization of sPP from the melt.[33] Figure 4(b) showed the time sequence of the optical micrographs of the sPP spherulites crystallized at 100 °C, which is strikingly similar to what we have demonstrated in the two-dimensional (2D) simulations. The initial nuclei grow into rectangular shape lamellae, reflecting the crystallographic axes of sPP crystals. These lamellae tend to stacked into lamellar bundles that transform to the sheaflike structure before emerging to dense lamellar branching morphology. Some spherulites show anisotropic nuclei with dual eye-pocket appearance at the core. In the case of multiple nucleations, the neighboring spherulites impinge and form the interface boundary. The heat released at the peripheral of the spherulite boundaries cannot escape since there is virtually no thermal gradient between the adjacent boundaries which themselves are heat sources. It is reasonable to infer that the present modified phase field model captures the sequential growth of the anisotropic nuclei leading to lamellar stacks, sheaflike, then to spherulites, and impingement of spherulites. These calculated morphological patterns are consistent with the experimental findings of the isothermal crystallization of sPP.

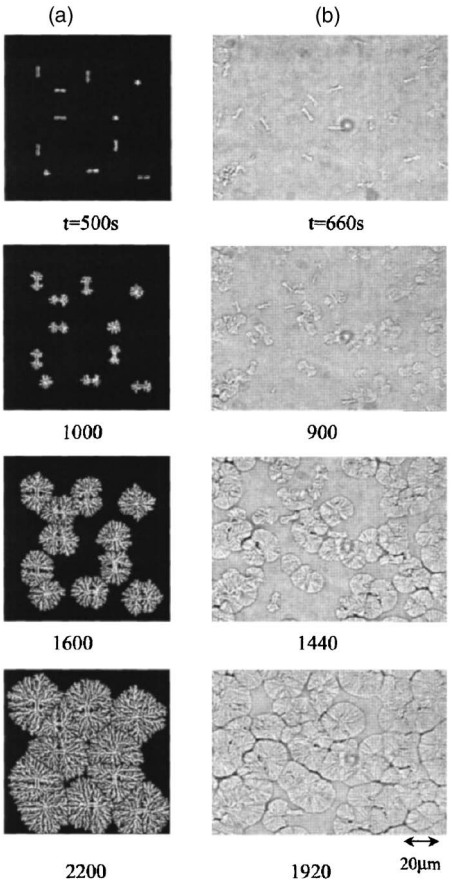

FIG. 4. (a) Spatiotemporal growth of multiple spherulites crystallized in the crystal order-parameter field with the grid size of 1024×1024, exhibiting the dense lamellar branching morphology. The length scale of the frame is 102.4 μm. (b) Time evolution of the spherulitic structure of the neat sPP at an isothermal crystallization temperature of 100 °C.

CONCLUSIONS

In summary, the present paper is the first to apply the modified phase field model for polymer crystallization to the elucidation of the imperfect polycrystalline nature of the emerged crystal morphology such as the dense branching morphology. In the 2D simulations of the spatiotemporal growth of the crystal order parameter under the self-generated thermal field, it is striking to discern the anisotropic nucleus with the lamellar stacks at the core of the spherulite that transform to sheaflike, and eventually to the lamellar branching morphology with the dual-eye-pocket-like texture. It is evident that the growth was controlled by the flux of latent heat, especially in generating the well-known lamellar branching morphology. In the case of multi-nuclei, the spherulites with the anisotropic lamellar stacks can be discerned. When impingement occurs, the grain boundaries form between the neighboring spherulites, which is in good accord with the experimental observations of spherulititic growth of sPP.

ACKNOWLEDGMENTS

Support of this work by NSF—DMR 02-09272, CRDF RC2-2398-02, and Ohio Board of Regent Research Challenge Grant is gratefully acknowledged. The authors are indebted to Dr. Leonid Manevitch and Dr. Elina Zubova, Semenov Institute of Chemical Physics, Russian Academy of Sciences, Moscow, for the fruitful discussion and constructive suggestions.

APPENDIX: DERIVATION OF DYNAMICS OF CRYSTAL NUCLEATION AND GROWTH

To derive the thermal influence on the interface structure development observed in the solidification process,[26] a convenient place to start is the Gibbs-Thomson equation. For one-component system the Gibbs-Thomson equation may be expressed as

$$\frac{\nu_n}{\mu_k} = T_m - T - \gamma\kappa, \tag{A1}$$

where μ_k is the kinetic coefficient, γ is the Gibbs-Thomson coefficient, ν_n is the speed of the advancing interface which can be related to the average unit normal vector of the propagating solid-liquid interface, defined as $\boldsymbol{n}=-\nabla\psi/|\nabla\psi|$ which is normal to the solid-melt boundary, defined as

$$\nu_n = \boldsymbol{v}_i\cdot\boldsymbol{n} = \frac{\partial x}{\partial t}\left(\frac{\partial\psi/\partial x}{|\nabla\psi|}\right) = \frac{\partial\psi/\partial t}{|\nabla\psi|}. \tag{A2}$$

On the other hand, the coefficient of the interface curvature gradient κ, is given as

$$\kappa = \nabla\cdot\boldsymbol{n} = -\frac{1}{|\nabla\psi|}\left[\nabla^2\psi - \frac{(\nabla\psi)\,.\,\nabla|\nabla\psi|}{|\nabla\psi|}\right]. \tag{A3}$$

Substituting Eqs. (A2) and (A3) into Eq. (A1), one obtains

$$\frac{\partial\psi}{\partial t} = \nu_n|\nabla\psi| = \mu_k\gamma\left[\nabla^2\psi - \frac{(\nabla\psi)\,.\,\nabla|\nabla\psi|}{|\nabla\psi|}\right] + \mu_k(T_m - T)|\nabla\psi|. \tag{A4}$$

According to Beckermann *et al.*,[26] the second term in the full bracket on the right-hand side of Eq. (A4) can be expressed in term of the double-well potential as

$$\frac{(\nabla\psi)\,.\,\nabla|\nabla\psi|}{|\nabla\psi|} = \psi(\psi-1)(2\psi-1). \tag{A5}$$

An analogous expression of Eq. (A5) may be written in the form of Kobayashi's double-well potential for a small molecule system[10] as

$$\frac{(\nabla\psi)\,.\,\nabla|\nabla\psi|}{|\nabla\psi|} = W\psi(\psi-1)(\psi-\zeta), \tag{A6}$$

setting $W=2$ and $\zeta=\frac{1}{2}$ at equilibrium. For polymer crystals, the right-hand side of Eq. (A6) may be written in a more general form as $W\psi(\psi-\zeta_0)(\psi-\zeta)$, where ζ_0 is the limiting crystal order parameter (i.e., the maximum linear crystallinity or folded chain length) for a given supercooling during polymer crystallization. Similarly, the last term in Eq. (A4) can be can be interpreted as the thermal force at the interface,

$$\eta = \mu_k(T_m - T)|\nabla\psi|. \tag{A7}$$

This thermal force at the interface serves as a heat source as well since it relates directly to the latent heat. If one utilizes a double-well potential for the local free energy, the steady-

state solution for the phase field equation leads to[10]

$$\psi = \frac{1}{2}\left(1 - \tanh\frac{n}{2\delta}\right), \tag{A8}$$

where n is the normal to interface and "δ" is a measure of the interface thickness. Then after a few mathematical deductions from Eq. (A6) one obtains

$$|\nabla\psi| = \frac{\partial\psi}{\partial n} = \frac{\psi(1-\psi)}{\delta}. \tag{A9}$$

For polymer crystals Eq. (A9) may be written as $|\nabla\psi| = \psi(\zeta_0 - \psi)/\delta$. Physically, Eqs. (A7) and (A9) imply that the thermal force, which itself is a heat source, is operative only at the solid-liquid interface. Substituting Eqs. (A9) and (A7) into Eq. (A4), one obtains

$$\frac{\partial\psi}{\partial t} = -\mu_k\gamma[W\psi(\psi-\zeta_0)(\psi-\zeta) - \nabla^2\psi] + (\mu_k/\delta)(T_m - T)\psi(\zeta_0 - \psi). \tag{A10}$$

Thus the first term of (A10) is analogous to the time evolution equation Eq. (5) which is similar to those of Chan[14] and/or Harrowell-Oxtoby.[19] The second term is the thermal force at the solid-melt interface which was introduced in an *ad hoc* manner at the interface by Kobayashi,[10] viz., $\eta(\psi) = \mu\psi(1-\psi)$.

[1] P. H. Geil, *Polymer Single Crystals*, 2nd ed. (Krieger, New York, NY, 1973).
[2] J. M. Marentette and G. R. Brown, J. Chem. Educ. **70**, 435 (1993).
[3] J. J. Point, Bull. Acad. R. Med. Belg. **41**, 982 (1955).
[4] H. D. Keith and F. J. Padden, Jr., J. Appl. Phys. **35**, 1270 (1964).
[5] A. Keller, J. Polym. Sci. **17**, 351 (1955).
[6] A. Keller, J. Polym. Sci. **36**, 361 (1959).
[7] F. P. Price, J. Polym. Sci. **37**, 71 (1959).
[8] H. D. Keith and F. J. Padden, Jr., J. Appl. Phys. **34**, 2409 (1963).
[9] G. Caginalp and P. C. Fife, Phys. Rev. B **33**, 7792 (1986); G. Caginalp, Arch. Ration. Mech. Anal. **92**, 205 (1986).
[10] R. Kobayashi, Physica D **63**, 410 (1993).
[11] A. A. Wheeler, W. J. Boettinger, and G. B. Mcfadden, Phys. Rev. A **45**, 7424 (1992).
[12] T. Kyu, R. Metha, and H.-W. Chiu, Phys. Rev. E **61**, 4161 (2000).
[13] L. D. Landau and E. M. Lifshitz, *Statistical Physics* (Pergamon, London, 1958), Chaps. 12 and 14.
[14] S. K. Chan, J. Chem. Phys. **67**, 5755 (1977).
[15] J. D. Hoffman and J. I. Lauritzen, Jr., J. Res. Natl. Bur. Stand., Sect. A **65**, 297 (1961).
[16] J. D. Hoffman and J. J. Weeks, J. Res. Natl. Bur. Stand., Sect. A **66**, 13 (1962).
[17] S. M. Allen and J. W. Cahn, Acta Metall. **27**, 1085 (1979).
[18] R. Mehta, W. Keawwattana, and T. Kyu, J. Chem. Phys. **120**, 4024 (2004).
[19] P. R. Harrowell and D. W. Oxtoby, J. Chem. Phys. **86**, 2932 (1987).
[20] *Polymer Handbook*, 4th ed., edited by J. Brandrup and E. H. Immergut (Wiley-Interscience, New York, 1999).
[21] J. W. Cahn and J. E. Hilliard, J. Chem. Phys. **28**, 258 (1958).
[22] P. J. Flory, *Principles of Polymer Chemistry* (Cornell University Press, Ithaca, 1953) Chap. 12.
[23] A. A. Wheeler, W. J. Boettinger, and G. B. Mcfadden, Phys. Rev. A **45**, 7424 (1992).
[24] K. R. Elder, F. J. Drolet, M. Kosterlitz, and M. Grant, Phys. Rev. Lett. **72**, 677 (1994).
[25] T. Kyu, H.-W. Chiu, A. J. Guenthner, Y. Okabe, H. Saito, and T. Inoue, Phys. Rev. Lett. **83**, 2749 (1999).
[26] C. Beckermann, H. J. Diepers, I. Steinbach, A. Karma, and X. Tong, J. Comput. Phys. **154**, 468 (1999).
[27] W.-G. Hu, C. Boeffel, and K. Schmidt-Rohr, Macromolecules **32**, 1611 (1999).
[28] K. Kuwabara, H. Kaji, M. Tsuji, and F. Horii, Macromolecules **33**, 7093 (2000).
[29] L. Granasay, T. Pusztai, T. Borzsonyi, J. A. Warren, and J. F. Douglass, Nat. Mater. **3**, 645 (2004).
[30] K. Taguchi, H. Miyaji, K. Izumi, A. Hoshino, Y. Miyamoto, and R. Kokawa, Polymer **42**, 7443 (2001).
[31] H. Xu, R. Matkhar, and T. Kyu, Phys. Rev. E **72**, 011804 (2005).
[32] H. Xu, Ph.D. dissertation, University of Akron, Akron, OH, 2004.
[33] W. Keawwattana, Ph.D. dissertation, University of Akron, Akron, OH, 2002.
[34] L. Li, C. M. Chan, J. X. Li, K. M. Ng, and Y. G. Lei, Macromolecules **32**, 8240 (1999).

The Journal of Chemical Physics is copyrighted by the American Institute of Physics (AIP). Redistribution of journal material is subject to the AIP online journal license and/or AIP copyright. For more information, see http://ojps.aip.org/jcpo/jcpcr/jsp